Current Biology 20, 1048–1052, June 8, 2010 ©2010 Elsevier Ltd All rights reserved DOI 10.1016/j.cub.2010.04.025

Report

Functional Comparison of H1 Histones in *Xenopus* Reveals Isoform-Specific Regulation by Cdk1 and RanGTP

Benjamin S. Freedman[1] and Rebecca Heald[1,*]
[1]Molecular and Cell Biology Department, University of California, Berkeley, Berkeley, CA 94720-3200, USA

Summary

H1 "linker" histones bind dynamically to nucleosomes and promote their compaction into chromatin fibers [1–4]. Developmental H1 isoforms are evolutionarily conserved, but their function, regulation, and posttranslational modifications are poorly understood [5–7]. In *Xenopus* egg extracts, the embryonic linker histone H1M does not affect nuclear assembly or replication but is required for proper chromosome architecture during mitosis [8, 9]. We report here that somatic H1 isoforms, which are more positively charged and feature multiple Cdk1 phosphorylation sites, cannot substitute for H1M at endogenous concentrations, instead causing chromatin compaction during interphase and dissociating from chromosomes at the onset of mitosis. Mitotic Cdk1 phosphorylation is not responsible for this dissociation and instead functions to enhance H1 binding in egg extracts and embryos. Nuclear import receptors RanBP7 and importin β bind tightly to somatic H1 but not H1M, and addition of a constitutively active Ran mutant abolishes this interaction and enhances the ability of somatic H1 to rescue mitotic chromosome architecture. Our results reveal distinct regulatory mechanisms among linker histone isoforms and a specific role for H1M to compact chromosomes during egg meiotic arrest and early embryonic divisions.

Results and Discussion

Somatic H1 Cannot Substitute for H1M at Endogenous Concentrations

We showed previously that immunodepletion of H1M from egg extracts results in elongated mitotic chromosomes that align poorly in the spindle and are consistently about 2-fold longer and 30% thinner than controls in the same extract [10]. A strong rescue of chromosome morphology and H1M immunofluorescence required 1 μM recombinant H1M, which is equivalent to the endogenous concentration in the egg, whereas lower concentrations yielded partial rescues in a dose-dependent manner (see Figures S1A and S1B available online; data not shown). To test the functional equivalence of developmental H1 isoforms, we generated recombinant, 6xHistidine-tagged H1M, H1A, or H10 proteins with *X. tropicalis* clones (to avoid allelic variants in the pseudotetraploid *X. laevis*). H1A typifies the replication-dependent linker histones present in most metazoan cells, whereas H10 is specific to differentiated cell types [5–7]. Both are smaller and more basic than H1M, contain 4–5 consensus Cdk1 phosphorylation sites in their C-terminal domains, and behaved more similarly to one another than to H1M; they will therefore be referred to collectively as "somatic H1." Surprisingly, unlike H1M, somatic H1 failed to rescue the elongated mitotic chromosome phenotype at concentrations of 1–2 μM (Figures 1A and 1B) and could restore mitotic chromosome morphology only at 3.5 μM (Figure 1C). Although we previously reported that H1 purified from calf thymus, which is 54% identical to somatic H1A, could rescue H1M-depleted mitotic chromosome compaction similarly to H1M [10], protein concentrations were approximate. In this study, precise protein concentrations were determined by Coomassie staining of a dilution series in comparison with known mass standards (data not shown), and equal amounts were added to H1M-depleted egg extracts, as confirmed by immunoblot analysis of the 6xHistidine tag (Figure S1C). Indeed, upon repeating the experiment, we found that chromosome morphology was not restored with 1.3 μM calf thymus H1 but required concentrations above 3 μM, comparable to recombinant H1A (Figure S1D; data not shown). The quantification of dose dependence and detailed morphometric analyses presented here were essential to distinguish differences among H1 proteins.

Somatic H1 Dissociates from Mitotic Chromosomes but Compacts Interphase Chromatin

To determine whether the failure of somatic H1 to rescue morphology reflected reduced mitotic chromosome binding, we performed immunofluorescence analysis of the recombinant 6xHistidine tag on samples of nuclei and mitotic chromosomes to compare its localization during interphase and mitosis (Figure 2A). Both somatic H1 and H1M localized to interphase nuclei, but a striking reduction in somatic H1 was observed on mitotic chromosomes, which could also be detected by comparing chromatin isolated from interphase and mitotic extracts by immunoblot (data not shown). We confirmed this dynamic localization pattern by fluorescence time-lapse analysis of individual nuclei, which showed that 1.5 μM Alexa 488-labeled somatic H1, but not H1M, dissociated from chromatin shortly after nuclear envelope breakdown (Movies S1 and S2). This analysis indicated that somatic H1 isoforms do not bind well to chromatin during mitosis but do associate with interphase chromatin. In fact, the chromatin binding and compacting activity of somatic H1 during interphase was greater than that of H1M. Whereas interphase chromatin remained diffuse within the nucleus when 1.8 μM H1M was added, the same amount of somatic H1 hypercompacted chromatin and produced bright foci connected by thin fibers of 0.81 ± 0.11 μm width (Figure 2B). At the higher concentration of 3.5 μM, H1M also caused hypercompaction, which resembles an H1 overexpression phenotype reported in somatic cells [11]. In summary, somatic H1 compacts interphase chromatin at lower concentrations than H1M but requires significantly higher concentrations to associate with and condense metaphase chromosomes (see schematic in Figure 2C).

Somatic H1 Binding to Mitotic Chromosomes Is Enhanced by Cdk1 Phosphorylation

Cyclin-dependent kinase (Cdk1) phosphorylates somatic H1 isoforms, but not H1M, at multiple sites and has been proposed to reduce H1 binding to chromatin [12]. We therefore hypothesized that this posttranslational modification could be responsible for the dissociation of somatic H1 from mitotic

*Correspondence: bheald@berkeley.edu

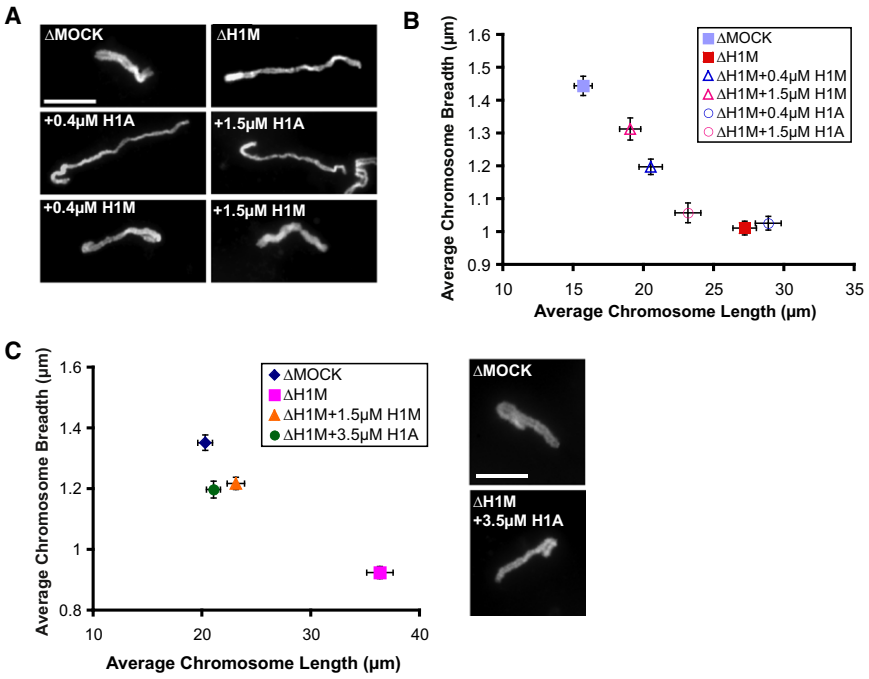

Figure 1. Somatic H1 Cannot Substitute for H1M at Endogenous Concentrations

(A) Individual chromosomes assembled in mock-depleted (ΔMOCK) or H1M-depleted (ΔH1M) extracts or in H1M-depleted extracts supplemented with 0.4 μM or 1.5 μM H1M or H1A. H1M consistently rescued more efficiently than H1A, even at lower concentrations.

(B) Quantification of chromosome morphology from the experiment described in (A). Images of individual chromosomes (n > 30) were thresholded, and their average fiber lengths and breadths were calculated and plotted.

(C) 3.5 μM somatic H1 rescues H1M-depleted chromosome morphology similar to a lower concentration of H1M. Average lengths and breadths of individual chromosomes (n > 40) and representative chromosomes are shown. Because somatic H1 causes interphase compaction at this concentration, H1 proteins were added only at the onset of mitosis. Scale bars represent 10 μm; error bars represent standard error. See also Figure S1.

chromosomes in egg extract, which contains high Cdk1 activity. We generated a mutant somatic H1 protein, in which the consensus Cdk1 phosphorylation serines (SPxK amino acid motif) were mutated to alanines, and confirmed that it was not phosphorylated in an extract kinase assay (Figure 3A). If Cdk1 phosphorylation causes H1 dissociation, this mutant should be retained on mitotic chromosomes. However, when added to metaphase reactions, the nonphosphorylatable mutant localized to chromosomes even less intensely than either wild-type H1 or a phosphomimetic mutant, in which the serines were substituted with glutamic acid residues (Figure 3B). Reduced chromatin binding of nonphosphorylatable somatic H1 was specific to mitosis and did not depend on nuclear assembly or H1 import, because similar results were obtained upon addition of GFP-tagged proteins to metaphase cytostatic factor-arrested (CSF) egg extracts in which sperm nuclei were directly remodeled into mitotic chromatin without an intervening interphase (Figure 3C). Phosphorylation site mutations also did not improve somatic H1 function at concentrations of 1–2 μM, which still failed to rescue H1M-depleted chromosome morphology (data not shown). Thus, mitotic Cdk1 phosphorylation cannot be responsible for the dissociation of somatic H1 from mitotic chromosomes in *Xenopus* egg extracts.

It was important to determine whether differences between H1 isoforms and mutants observed in egg extracts also hold true in somatic cells. We therefore investigated linker histone localization during mitosis in *Xenopus* embryos, where somatic H1 is normally expressed. H1A accumulated only after the midblastula transition (stage 8), consistent with previous reports [11, 13, 14], and appeared to localize brightly to mitotic chromosomes (Figures S2A and S2B). To directly compare mitotic chromosome binding of isoforms and phosphorylation site mutants, we exogenously coexpressed H1M- or H1A-GFP

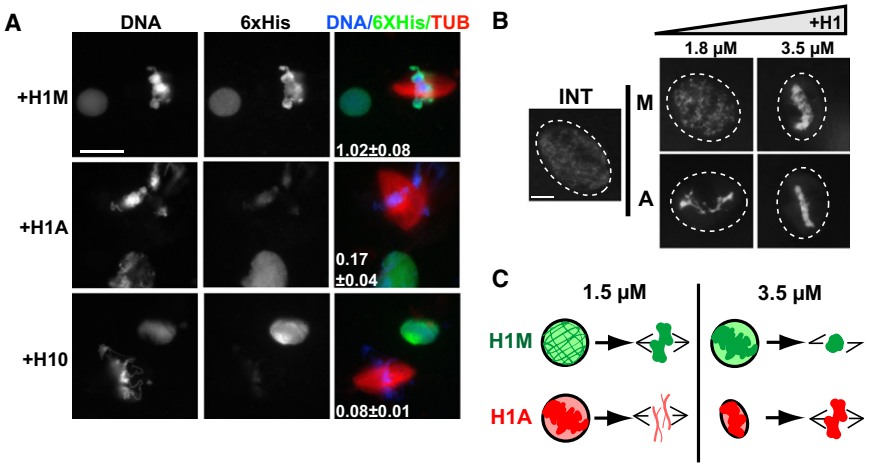

Figure 2. Somatic H1 Dissociates from Mitotic Chromosomes

(A) Anti-6xHistidine immunofluorescence of nuclei and mitotic spindles from H1M-depleted reactions supplemented with 1 μM of 6xHistidine-tagged H1M, H10, or H1A. Interphase and mitotic reactions were separately diluted into a fixation buffer, then mixed and spun onto a single coverslip for staining. The average H1:DNA (6×Histidine:Hoechst, ±standard error) fluorescence intensity of mitotic chromosome clusters (5–15 per condition) divided by that of interphase nuclei is shown for each condition in the merged image. Scale bar represents 25 μm.

(B) Nuclei assembled in undepleted reactions supplemented with increasing concentrations of H1M (left) or H1A (right). Only H1A causes chromatin compaction at the lower dose (>30 nuclei analyzed per condition). Scale bar represents 10 μm.

(C) Schematic showing functional effects of two different concentrations of H1M and H1A during interphase and mitosis. See also Movies S1 and S2.

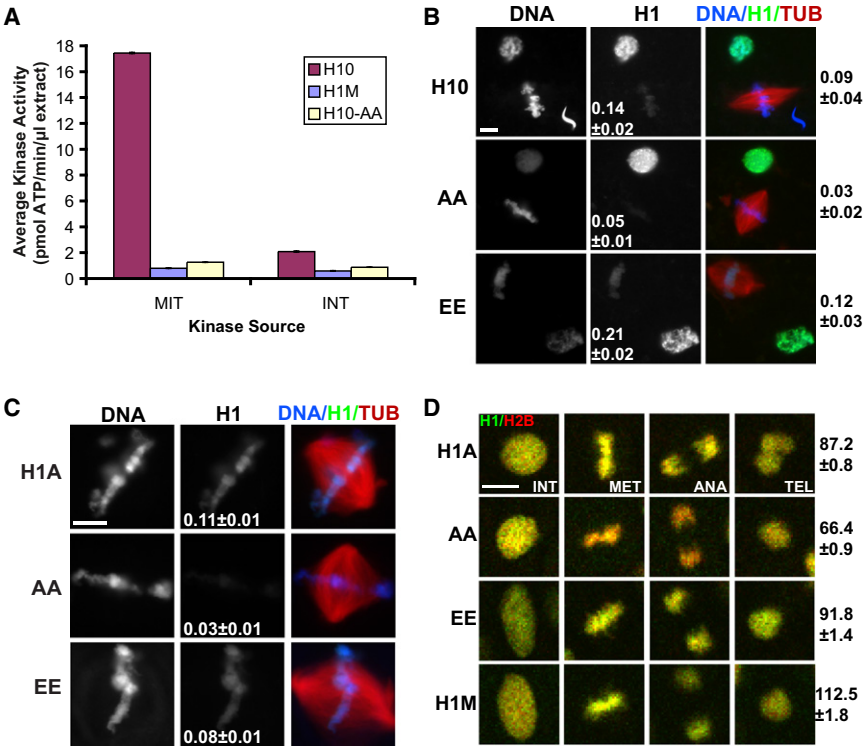

Figure 3. Somatic H1 Chromosome Binding Is Enhanced by Phosphorylation

(A) H1 kinase assay from metaphase cytostatic factor (CSF)-arrested (MET) or interphase (INT)-arrested egg extracts for H1M, H10, and alanine-substituted H10 (-AA).

(B) Anti-6xHistidine immunofluorescence of reactions with H10 wild-type versus alanine (AA) or glutamic acid (EE) phosphorylation site mutants. Interphase or mitotic reactions were fixed separately, then mixed and processed together. Average H1:DNA (6xHistidine:Hoechst) fluorescence ratio is shown for mitotic chromosomes alone (center) or mitotic chromosomes over interphase nuclei (right, ±standard error).

(C) Sperm nuclei were remodeled directly into mitotic chromosomes in CSF egg extracts supplemented with 1 μM H1A-GFP or phosphorylation site mutants, and the average H1:DNA (GFP:DAPI) fluorescence ratio was determined (center, ±standard error).

(D) Time-lapse images of dividing cells in stage 13 embryos expressing H1-GFP (green) and H2B-RFP (red). The Cdk1 phosphorylation site alanine mutant (AA) binds to mitotic chromosomes with reduced affinity compared to wild-type H1A, H1A-EE, or H1M, causing chromatin to shift from yellow to red. H1-GFP signal was normalized to H2B-RFP levels for single cells at interphase and anaphase, and the anaphase:interphase fluorescence ratio was calculated for each individual cell and averaged (right, ±standard error). Scale bars represent 10 μm. Ten to fifty structures or cells were examined per condition. See also Figure S2 and Movies S3–S5.

fusion proteins with histone H2B-RFP in neurula (stage 13–15) embryos and examined them by confocal fluorescence time-lapse microscopy, allowing quantification of histone fluorescence intensity on chromosomes in single cells as they underwent mitosis (Figure 3D; Movies S3–S5). Although GFP-tagged H1 proteins were similarly bright during interphase (Figure S2C; data not shown), we found that the intensity of H1A-GFP relative to H2B-RFP decreased transiently during mitosis to ~85% of interphase levels (Movie S3), whereas H1M-GFP binding increased to ~110% (Movie S4). Mutation of Cdk1 phosphorylation sites to alanines further decreased H1A-GFP binding to ~65% of interphase levels (Movie S5), whereas mutation to glutamic acids was comparable to wild-type (Figure 3D). In addition, fluorescence recovery after photobleaching of the alanine substitution mutant during mitosis was significantly faster than that of wild-type H1A-GFP or the phosphomimetic mutant, and fluorescence recovered to a slightly higher extent, suggesting that unphosphorylated H1 has a higher off rate from chromatin and a greater mobile fraction (Figure S2D). These data suggest that relative differences between H1 isoforms at mitosis persist in somatic cells but that somatic H1 dissociation occurs to a lesser degree and is reversed by Cdk1 phosphorylation. Even though somatic H1 binding to mitotic chromosomes was lower in egg extracts than in embryos, the relative affinities of phosphorylation site mutants were similar (Figures 3B–3D), indicating that H1 phosphorylation is a general mechanism that increases its binding to mitotic chromosomes.

Nuclear Import Receptors Bind and Inhibit Somatic H1 during Mitosis

An important question is why somatic H1, but not H1M, dissociates from chromosomes at mitosis. Having ruled out somatic H1-specific phosphorylation by Cdk1, we performed pull-downs from egg extracts with recombinant GST-H1 fusion proteins to discover other potential mechanisms. Somatic H1, but not H1M, strongly associated with proteins of 90 kDa and 110 kDa, which mass spectrometry analysis revealed to be importin β and RanBP7 (Ran-binding protein 7 or importin-7), respectively (Figure 4A). A 95 kDa protein, Eef2 (eukaryotic translation elongation factor 2), frequently appeared in both H1M and somatic H1 pull-downs, but we have not determined whether this is a specific interaction. An importin β/RanBP7 heterodimer was previously reported to mediate nuclear import of somatic H1, releasing the H1 cargo upon binding to RanGTP in the nucleus [15, 16]. Consistent with this regulatory mechanism, we found that addition of 15 μM RanQ69L, a mutant locked in the GTP-bound state, disrupted binding of importin β/RanBP7 to somatic H1 in egg extracts (Figure 4A). To determine what regions of somatic H1 associate with importins, we performed pull-downs with H1M/H10 chimeras, in which the head of one isoform was fused to the tail of the other, and found that all combinations interacted with importin β/RanBP7, indicating that multiple regions of somatic H1 contribute to importin binding (Figure S3A). Mutation of somatic H1 Cdk1 phosphorylation sites did not have a detectable effect on its interaction with importin β/RanBP7 in pull-down assays (Figure S3B). Although H1M did not appear to bind tightly to these receptors, fluorescently tagged H1M underwent active nuclear import at rates that appeared to be slower than GFP-H1A (data not shown).

Our laboratory and others have previously shown that importin β functions during mitosis to bind and inhibit spindle assembly factors, raising the possibility that importin β/RanBP7 might similarly inhibit somatic H1. Importin β inhibition of spindle assembly factors is reduced in the immediate

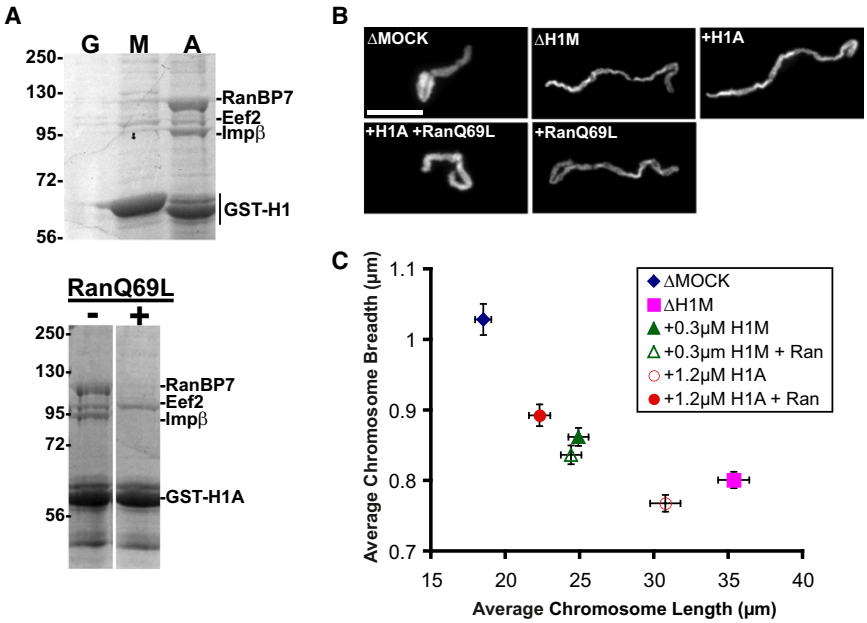

Figure 4. RanGTP Releases Somatic H1 from Nuclear Import Receptors and Promotes Its Chromosome Binding

(A) Top: Coomassie-stained gel of proteins pulled down with GST (G) or H1M- and H1A-GST fusion proteins (M, A) from metaphase-arrested extract. GST (22 kDa) is not shown. Bottom: GST-H1A pull-downs supplemented with 15 μM RanQ69L (+) or buffer control (−).

(B) Representative mock- or H1M-depleted chromosomes assembled with or without recombinant H1A (1.2 μM) and RanQ69L (15 μM). A subpopulation of unrescued chromosomes was also observed in the +H1A +RanQ69L condition but is not shown. Scale bar represents 10 μm.

(C) Average chromosome morphology (n > 30 per condition) comparing the effects of RanQ69L with either 1.2 μM H1A or 0.3 μM H1M. Doses were chosen that could not rescue chromosome morphology on their own. Error bars represent standard error. See also Figure S3.

vicinity of mitotic chromosomes, where a gradient of RanGTP arises as a result of the presence of the chromatin-bound RanGEF, RCC1 [17, 18]. To test whether importin β/RanBP7 regulates the chromatin binding and activity of somatic H1, we added RanQ69L to extract reactions at the onset of mitosis. Ectopic generation of microtubules indicated that mitotic cargoes of importin β were released (data not shown; [17]). Morphometric analysis showed that addition of RanQ69L and somatic H1 together, but not individually, gave a substantial rescue of mitotic chromosome morphology. Significantly, this effect was specific to somatic H1, because RanQ69L did not enhance a partial rescue of chromosome structure by H1M (Figures 4B and 4C). Averaged over three experiments, adding somatic H1 or RanQ69L individually resulted in chromosomes that were 71% ± 10% or 79% ± 9% longer than mock depletes, respectively, whereas adding both factors yielded chromosomes only 22% ± 7% longer. These data suggest that the binding and compaction activity of somatic H1 on mitotic chromosomes is inhibited by importin β/RanBP7, and this inhibition is relieved in the presence of RanGTP. Although the rescue was substantial, it was not complete, indicating that other mechanisms may also regulate somatic H1.

Altogether, our comparison of H1 isoforms suggests a model for their function during the cell cycle in egg extracts (Figure S3C). H1M interacts only weakly with importin β/RanBP7 and binds efficiently to both interphase and mitotic chromatin. Somatic H1, which is more positively charged, interacts strongly with importin β/RanBP7. In interphase nuclei, RanGTP concentrations are very high, releasing somatic H1 from these receptors and promoting its chromatin binding. Following nuclear envelope breakdown, concentrations of somatic H1 and RanGTP surrounding chromatin are reduced by diffusion. Although a steep gradient of RanGTP persists around mitotic chromosomes in egg extracts [18], a significant pool of linker histone does not colocalize, and stoichiometric concentrations of somatic H1 may not be released from the receptors, thereby reducing chromatin binding and compaction during mitosis relative to interphase. Phosphorylation of somatic H1 by Cdk1 on multiple sites, which has been a mystery for over 30 years, functions to strengthen H1 binding to mitotic chromosomes and offset dissociation. This makes sense given that linker histones function to compact chromatin, and this occurs maximally during mitosis. The effects of somatic H1 phosphorylation were evident by single-cell analysis in the embryo, where it is normally expressed, and did not appear to reduce the interaction with importin β/RanBP7. Whether and how importin β/RanBP7 and RanGTP contribute to somatic H1 regulation in the context of the embryo is an open question that is difficult to address given the general import role of these factors and given the fact that positively charged residues throughout somatic H1 contribute to importin β/RanBP7 binding. It is tempting to speculate that because the mitotic RanGTP gradient occupies a larger proportion of the cytoplasmic volume in somatic cells [19], more H1 may be released from the importin β/RanBP7 heterodimer.

H1 isoforms and phosphorylation sites may have evolved to match different cellular conditions. In egg cytoplasm, H1M ensures that chromosomes cluster together at the metaphase plate to achieve the compact morphology required for efficient and accurate segregation. Consequently, this isoform is optimized for chromosome binding within the large cells of the early embryo. In contrast, somatic H1 may have evolved to perform interphase functions and to associate with chromosomes in cells with a higher nuclear:cytoplasmic volume ratio. In such cells, the mitotic chromosome-binding properties of H1M might be detrimental, and indeed, we have observed that H1M overexpression is highly toxic to embryos (unpublished data). Future work will investigate the contribution of phosphorylated somatic H1 to chromosome condensation in embryos and the consequences of its overexpression or replacement by other isoforms and mutants.

Experimental Procedures

CSF low-speed egg extracts were immunodepleted, reacted, and processed for immunofluorescence as described [9, 10, 20]. Live movies were obtained by spotting 5 μl of extract reaction onto a glass slide overlaid with an 18 mm × 18 mm coverglass. Recombinant H1/mutants were purified

from bacteria in phosphate-buffered saline plus 500 mM NaCl and added to extracts prior to sperm addition, except for in overexpression experiments, in which they were added only at mitosis. At mitosis, 15 μM RanQ69L or XB buffer was added. Antibodies included monoclonal anti-His (Clontech 631212) and custom rabbit polyclonals anti-H1M and anti-H1A (*X. laevis*, Covance Research Services). Pull-downs were performed with glutathione Sepharose 4B (GE Healthcare). mRNAs were generated with the mMessage mMachine SP6 kit (Ambion), and 500 pg H1A-GFP or 100 pg H1M-GFP mRNA was injected together with 500 pg H2B-RFP mRNA into one-cell stage embryos. Similar expression levels of H1-GFP were confirmed by immunoblot, and neurulae were imaged and photobleached on an inverted Zeiss confocal. Image analysis was performed with Metamorph and ImageJ. See Supplemental Experimental Procedures for details.

Supplemental Information

Supplemental Information includes Supplemental Experimental Procedures, three figures, and five movies and can be found with this article online at doi:10.1016/j.cub.2010.04.025.

Acknowledgments

We thank S. Zhou for mass spectrometry, P. Kalab for purification of RanQ69L, E. Kieserman for help with confocal microscopy and reagents, K. Miller for preliminary experiments, and T. Maresca for advice and reagents. We thank members of the Heald and Harland laboratories for reagents and helpful discussions, as well as K. Weis and Z. Cande for comments on the manuscript. R.H. is supported by the National Institutes of Health (GM057839).

Received: February 2, 2010
Revised: April 6, 2010
Accepted: April 12, 2010
Published online: May 13, 2010

References

1. Thoma, F., and Koller, T. (1977). Influence of histone H1 on chromatin structure. Cell *12*, 101–107.
2. Finch, J.T., and Klug, A. (1976). Solenoidal model for superstructure in chromatin. Proc. Natl. Acad. Sci. USA *73*, 1897–1901.
3. Lever, M.A., Th'ng, J.P., Sun, X., and Hendzel, M.J. (2000). Rapid exchange of histone H1.1 on chromatin in living human cells. Nature *408*, 873–876.
4. Misteli, T., Gunjan, A., Hock, R., Bustin, M., and Brown, D.T. (2000). Dynamic binding of histone H1 to chromatin in living cells. Nature *408*, 877–881.
5. Godde, J.S., and Ura, K. (2008). Cracking the enigmatic linker histone code. J. Biochem. *143*, 287–293.
6. Happel, N., and Doenecke, D. (2009). Histone H1 and its isoforms: Contribution to chromatin structure and function. Gene *431*, 1–12.
7. Izzo, A., Kamieniarz, K., and Schneider, R. (2008). The histone H1 family: Specific members, specific functions? Biol. Chem. *389*, 333–343.
8. Dasso, M., Dimitrov, S., and Wolffe, A.P. (1994). Nuclear assembly is independent of linker histones. Proc. Natl. Acad. Sci. USA *91*, 12477–12481.
9. Maresca, T.J., and Heald, R. (2006). Methods for studying spindle assembly and chromosome condensation in Xenopus egg extracts. Methods Mol. Biol. *322*, 459–474.
10. Maresca, T.J., Freedman, B.S., and Heald, R. (2005). Histone H1 is essential for mitotic chromosome architecture and segregation in Xenopus laevis egg extracts. J. Cell Biol. *169*, 859–869.
11. Dworkin-Rastl, E., Kandolf, H., and Smith, R.C. (1994). The maternal histone H1 variant, H1M (B4 protein), is the predominant H1 histone in Xenopus pregastrula embryos. Dev. Biol. *161*, 425–439.
12. Baatout, S., and Derradji, H. (2006). About histone H1 phosphorylation during mitosis. Cell Biochem. Funct. *24*, 93–94.
13. Dimitrov, S., Almouzni, G., Dasso, M., and Wolffe, A.P. (1993). Chromatin transitions during early Xenopus embryogenesis: Changes in histone H4 acetylation and in linker histone type. Dev. Biol. *160*, 214–227.
14. Saeki, H., Ohsumi, K., Aihara, H., Ito, T., Hirose, S., Ura, K., and Kaneda, Y. (2005). Linker histone variants control chromatin dynamics during early embryogenesis. Proc. Natl. Acad. Sci. USA *102*, 5697–5702.
15. Jäkel, S., Albig, W., Kutay, U., Bischoff, F.R., Schwamborn, K., Doenecke, D., and Görlich, D. (1999). The importin beta/importin 7 heterodimer is a functional nuclear import receptor for histone H1. EMBO J. *18*, 2411–2423.
16. Jäkel, S., Mingot, J.M., Schwarzmaier, P., Hartmann, E., and Görlich, D. (2002). Importins fulfill a dual function as nuclear import receptors and cytoplasmic chaperones for exposed basic domains. EMBO J. *21*, 377–386.
17. Nachury, M.V., Maresca, T.J., Salmon, W.C., Waterman-Storer, C.M., Heald, R., and Weis, K. (2001). Importin beta is a mitotic target of the small GTPase Ran in spindle assembly. Cell *104*, 95–106.
18. Kalab, P., Weis, K., and Heald, R. (2002). Visualization of a Ran-GTP gradient in interphase and mitotic Xenopus egg extracts. Science *295*, 2452–2456.
19. Kalab, P., Pralle, A., Isacoff, E.Y., Heald, R., and Weis, K. (2006). Analysis of a RanGTP-regulated gradient in mitotic somatic cells. Nature *440*, 697–701.
20. Murray, A.W. (1991). Cell cycle extracts. Methods Cell Biol. *36*, 581–605.